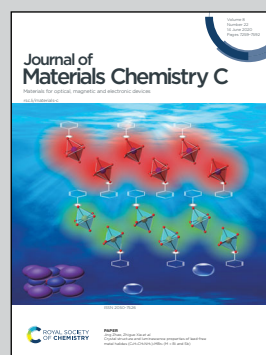


Showcasing collaborative research from Hoffmann Institute of Advanced Materials, China and Rutgers University, USA.

Zero-dimensional ionic antimony halide inorganic-organic hybrid with strong greenish yellow emission

A new zero-dimensional ionic antimony halide inorganic-organic hybrid structure was reported. It emits bright green-yellow light with high quantum efficiency, serving as a good example of lighting phosphors based on antimony halide hybrid materials.

As featured in:



See Wei Liu, Jing Li *et al.*,
J. Mater. Chem. C, 2020, **8**, 7300.

Cite this: *J. Mater. Chem. C*, 2020, **8**, 7300Received 28th October 2019,
Accepted 30th April 2020

DOI: 10.1039/c9tc05868k

rsc.li/materials-c

Zero-dimensional ionic antimony halide
inorganic–organic hybrid with strong greenish
yellow emission†Fang Lin,^a Hao Wang,^a Wei Liu^{a*} and Jing Li^{b*}

Here, we reported a new zero-dimensional ionic antimony halide inorganic–organic hybrid structure, $\text{H}_3\text{SbBr}_6(\text{L})_6$ ($\text{L} = 2\text{-(3-methyl-1H-imidazol-3-ium-1-yl)acetate}$). The inorganic component is a molecular SbBr_6^{3-} anion with an octahedral geometry for the metal. Each individual anion is surrounded by six organic ligands. The compound emits bright green-yellow light with high quantum efficiency (IQY = 55% at $\lambda_{\text{ex}} = 360$ nm). Combined with its low toxicity and high stability, the title compound serves as a good example of lighting phosphors based on antimony halide hybrid materials.

As a relatively new general lighting technology, solid-state lighting (SSL) devices (e.g. light-emitting diodes (LEDs) and organic light-emitting diodes (OLEDs)) are much more energy efficient than conventional lighting sources, and are therefore considered as future lighting solutions.^{1,2} The simplest white LEDs (WLEDs) are prepared by coating a yellow light emitting phosphor onto a blue LED chip. Commercial phosphors currently used in WLEDs are inorganic materials containing rare-earth elements (REEs). The dependence on REEs, in particular europium, terbium, and yttrium, can become problematic due to potential supply risk and cost issues, as well as their serious environmental impact.³ As a result, new types of REE-free lighting materials are in great demand.

Luminescent crystalline inorganic–organic hybrid materials have attracted tremendous attention recently due to their potential in display and lighting related applications.^{4–9} These materials are composed of either neutral or ionic inorganic and organic modules, and the two components are connected by either covalent or ionic bonds.^{10,11} Due to the incorporation of

both inorganic and organic component in a single crystal lattice, the hybrid structures show structural versatility and unique optical properties.^{12–15}

Antimony halide-based inorganic–organic hybrid materials have attracted much attention recently.^{16–18} They can be the non-toxic alternatives for lead halide structures for photovoltaic and lighting applications. Some members of this group exhibit very strong luminescence, showing great potential for highly efficient lighting phosphors.¹⁷ Huang *et al.* reported a highly yellow-emitting antimony-based hybrid structure, $[\text{Bmim}]_2\text{SbCl}_5$, with a high IQY of 86.3% in the solid state ($\text{Bmim} = 1\text{-butyl-3-methylimidazolium}$).¹⁶ Later, they reported two hybrid chloroantimonates showing thermally induced reversible luminescence and $[\text{Bzmim}]_3\text{SbCl}_6$ was reported to exhibit a green emission with an IQY of 87.5% ($\text{Bzmim} = 1\text{-benzyl-3-methylimidazolium}$).¹⁹ Ma *et al.* reported a 0D orange-emitting Sb halide-based hybrid structure, $(\text{C}_9\text{NH}_{20})_2\text{SbCl}_5$, with an exceptionally high PLQE of up to 98%.¹⁷ Another sample reported by the same group is $(\text{Ph}_4\text{P})_2\text{SbCl}_5$, which is a very efficient red phosphor, with a high IQY of 87%.²⁰ A direct white-light-emitting material from this family, $[4\text{-methylpiperidinium}]_2\text{SbCl}_5$, was also reported by Luo *et al.* with an IQY of $\sim 1\%$.¹⁸ An efficient white-light-emitting hybrid chloroantimonate, $(\text{TTA})_2\text{SbCl}_{5x}$, has been reported, with a high IQY of 68% ($\text{TTA} = \text{tetraethylammonium}$).²¹ Despite these findings, this type of hybrid structures and their luminescence are much less investigated compared to other types of hybrid systems.^{22–30} New structures with interesting luminescence properties from this family are of significant interest.

Here, we report the synthesis, characterization and luminescence properties of an antimony(III) containing inorganic–organic hybrid structure, namely $\text{H}_3\text{SbBr}_6(\text{L})_6$ ($\text{L} = 2\text{-(3-methyl-1H-imidazol-3-ium-1-yl)acetate}$) (**1**). The structure of the organic ligand is shown in Fig. S1 (ESI†). Bright green-yellow emission of **1** can be achieved under UV light irradiation, with the PL quantum yield (PLQY) as high as 55% in the solid state.

Compound **1** was prepared by solvothermal reaction of SbBr_3 , 1-carboxymethyl-3-methylimidazolium chloride and acetonitrile in a 20 mL Teflon-lined stainless-steel autoclave. The reaction

^a Hoffmann Institute of Advanced Materials, Shenzhen Polytechnic, 7098 Liuxian Blvd, Nanshan District, Shenzhen, 518055, China. E-mail: weilu2018@szpt.edu.cn

^b Department of Chemistry and Chemical Biology, Rutgers University, 123 Bevier Road, Piscataway, NJ, 08854, USA. E-mail: jingli@rutgers.edu

† Electronic supplementary information (ESI) available: Experimental details, PXRD patterns, DFT calculation results, UV-vis absorption spectra and PL spectra. CCDC 1960644. For ESI and crystallographic data in CIF or other electronic format see DOI: 10.1039/c9tc05868k

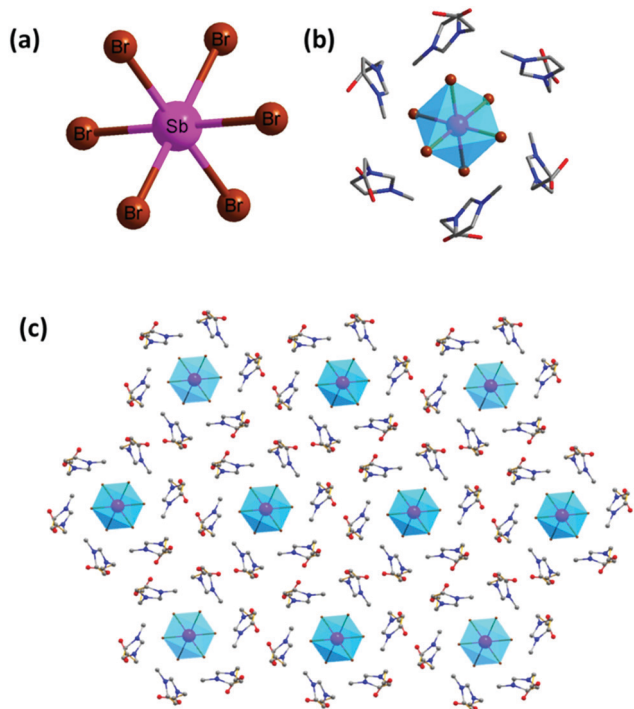


Fig. 1 (a) Structural plot of a metal halide octahedron, SbBr_6^{3-} . (b) Structural plot of the $\text{SbBr}_6(\text{L})_6^{3-}$ anion. (c) Structural plot of ten metal halide molecules and the surrounding ligands. (Pink balls: Sb atoms; dark red: Br atoms; red balls: O atoms; grey balls: C atoms; blue balls: N atoms; hydrogen atoms are hidden for clarity.)

was carried out at 120 °C for 4 days, affording colorless crystals of **1** in a yield of 56%. Single crystal X-ray diffraction analysis reveals that **1** crystallizes in the trigonal space group $R\bar{3}$ and the Sb ions are six-coordinated by Br in an octahedral geometry. The individual SbBr_6^{3-} octahedron is surrounded by organic ligands, as shown in Fig. 1. Detailed crystallographic data are summarized in Table S1 (ESI†). Though there are carboxylate groups in the organic ligands, they are not bonded to the Sb atoms. The phase purity of compound **1** was confirmed by powder X-ray diffraction analysis (PXRD) (Fig. S2, ESI†). The peak positions of the observed PXRD pattern are in good agreement with those simulated from single crystal X-ray data, indicating that a relatively pure phase is obtained. The compositions of the crystals were further verified by elemental analysis (Table S2, ESI†). Details of the synthesis and characterization can be found in the ESI†

The optical absorption spectrum for compound **1** was recorded at room temperature and converted to a Kubelka–Munk function, as shown in Fig. S3 (ESI†). The absorption edge for compound **1** was estimated to be ~ 2.8 eV. Thermal stability of the compound was evaluated by thermogravimetry (TG) analysis (Fig. S4, ESI†). The decomposition temperature (TD) of this compound was estimated to be 180 °C. Such a high TD compared to those of neutral hybrid molecular compounds is the result of the ionic bonding between the organic ligand and the inorganic component. The powder sample of **1** shows moderate air stability. The sample kept in a sample vial for one week shows almost no change in the PXRD pattern and emission intensity. Due to the

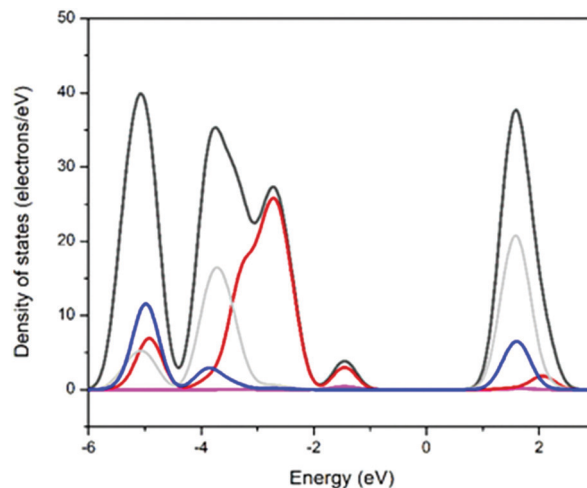


Fig. 2 Calculated density of states (DOS) of **1** by the DFT method: total DOS (black); Sb 4d orbitals (pink); Br 4p orbitals (dark red); C 2p orbitals (grey); N 2p orbitals (blue).

ionic nature of this compound, it would absorb water when placed in a moist environment.

First-principle calculations of the band structure (BS) and density of states (DOS) of compound **1** were carried out using the CASTEP code implemented in the Material studio 5.0 package, and the results are shown in Fig. 2 and Fig. S5 (ESI†). Generalized gradient approximations (GGAs) with the Perdew–Burke–Ernzerhof (PBE) exchange–correlation functional (xc) were used in all calculations. The plane-wave basis set energy cutoff was set at 10.0 eV, ultrasoft pseudopotentials were used for all chemical elements and the total energy tolerance was set to be 1×10^{-5} eV per atom. The calculated band structure of **1** shows a band gap of 2.73 eV. In Compound **1**, the main atomic states found in the region of the valence band (VB) maximum are Br 4p orbitals, with a small contribution from Sb 4d. The conduction band (CB) minimum region is populated predominantly by C 2p, with secondary contributions from N 2p orbitals. These observations indicate that the inorganic component (Sb and Br) dominates the VB maximum region, whereas in the region of the CB minimum, the major contribution is from the organic components. The band gaps of this type of compounds may be tuned by altering the halides or the structures of the organic ligands.

Single crystals of **1** are colorless and transparent under ambient light, suggesting almost no absorption in the visible region with a wide band gap. Under UV irradiation (360 nm), the crystals shine with bright green-yellow light (Fig. 3a). The room temperature emission and excitation spectra are shown in Fig. 3b. The green-yellow emission peak at 530 nm at room temperature had a full width at half-maximum (FWHM) of around 110 nm. Emissions under different excitation energies were also collected, and the results suggest that 360 nm is the optimal energy (Fig. S6, ESI†), which yielded the highest IQY value of 55%. This value is significantly higher than that of most other reported Sb-based hybrid structures.^{18,31–33} SbBr_3 and the organic ligands exhibit no emission under UV excitation (Fig. S7, ESI†). The fact that there is no bond between the inorganic and

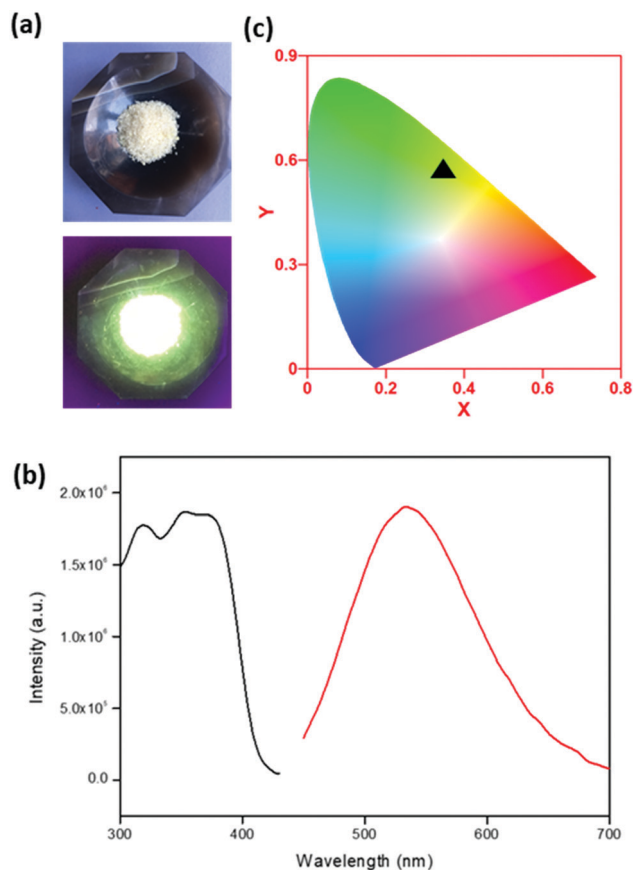


Fig. 3 (a) Sample images taken under natural light (top) and UV light (bottom); (b) excitation (black) and emission spectra (red) of **1**. $\lambda_{\text{ex}} = 360$ nm, and $\lambda_{\text{em}} = 530$ nm; (c) CIE coordinates of **1**.

organic components suggests that the bright green-yellow emission originates from the individual metal halide species. The Commission Internationale de l'Eclairage (CIE) chromaticity coordinates (Fig. 3c) for the emission were calculated to be (0.35, 0.55). Emission spectra at different temperatures were also obtained (Fig. S8, ESI[†]). It is interesting to note that emission intensity decreases as the temperature is lowered and the emission band becomes narrower. Also, the emission energies shift to the lower energy region as temperature decreases. The luminescence decay of this green-yellow emitter at room temperature is shown in Fig. S9 (ESI[†]), giving a long lifetime of approximately 2.15 μs by monoexponential fitting. This is consistent with what has been observed in other 0D organic metal halide hybrids with emissions from the excitons localized in individual metal halide species.¹⁷ The decay lifetimes in microseconds at both room temperature and 77 K suggest that they are phosphorescent emissions. The major photophysical properties of **1** have been summarized in Table 1.

Table 1 Summary of photophysical properties of **1**

| T (K) | λ_{ex} (nm) | λ_{em} (nm) | FWHM (nm) | IQY (360 nm) | τ (μs) |
|-------|----------------------------|----------------------------|-----------|---------------|--------------------------|
| 298 | 360 | 530 | 110 | 55% | 2.15 |
| 77 | 360 | 545 | 90 | Not available | 7.61 |

Conclusions

A new zero-dimensional ionic antimony halide inorganic-organic hybrid structure, $\text{H}_3\text{SbBr}_6(\text{L})_6$ ($\text{L} = 2\text{-(3-methyl-1H-imidazol-3-ium-1-yl)acetate}$), has been prepared by a solvothermal method. This metal halide compound expands the family of Sb-based hybrid structures. The inorganic component is anionic molecular (SbBr_6^{3-}) octahedra that are completely isolated from each other and surrounded by the organic ligands. Its bandgap was estimated to be ~ 2.73 eV from the experimental optical absorption measurements. While the atomic states populated in the VB maximum region are mainly from the inorganic elements (Sb and Br), the composition in the CB minimum is mainly from the organic (C and N) elements. This compound emits greenish yellow light ($\lambda_{\text{em}} = 530$ nm) in the solid state with a high internal quantum yield (IQY) of 55%. This compound serves as an example of highly luminescent antimony halide-based hybrid materials, potentially important for the development of eco-friendly lighting phosphors. The luminescence properties of the recently reported Sb-based hybrid structures have been summarized in Table S3 (ESI[†]) for comparison.

Conflicts of interest

There are no conflicts to declare.

Acknowledgements

Financial support from the National Natural Science Foundation of China (grant no. 21901167) and Shenzhen Science and Technology Innovation Commission (grant no. JCYJ20180307102051326) is gratefully acknowledged.

Notes and references

- 1 J. McKittrick and L. E. Shea-Rohwer, *J. Am. Ceram. Soc.*, 2014, **97**, 1327–1352.
- 2 X. Huang, *Nat. Photonics*, 2014, **8**, 748.
- 3 H. Zhu, C. C. Lin, W. Luo, S. Shu, Z. Liu, Y. Liu, J. Kong, E. Ma, Y. Cao, R.-S. Liu and X. Chen, *Nat. Commun.*, 2014, **5**, 4312.
- 4 W. Ki, J. Li, G. Eda and M. Chhowalla, *J. Mater. Chem.*, 2010, **20**, 10676–10679.
- 5 M.-S. Wang and G.-C. Guo, *Chem. Commun.*, 2016, **52**, 13194–13204.
- 6 K. Lin, J. Xing, L. N. Quan, F. P. G. de Arquer, X. Gong, J. Lu, L. Xie, W. Zhao, D. Zhang, C. Yan, W. Li, X. Liu, Y. Lu, J. Kirman, E. H. Sargent, Q. Xiong and Z. Wei, *Nature*, 2018, **562**, 245–248.
- 7 J. Liang, L. Ying, F. Huang and Y. Cao, *J. Mater. Chem. C*, 2016, **4**, 10993–11006.
- 8 E. R. Dohner, E. T. Hoke and H. I. Karunadasa, *J. Am. Chem. Soc.*, 2014, **136**, 1718–1721.
- 9 E. R. Dohner, A. Jaffe, L. R. Bradshaw and H. I. Karunadasa, *J. Am. Chem. Soc.*, 2014, **136**, 13154–13157.
- 10 J. Li and R. B. Zhang, *Comprehensive Inorganic Chemistry*, Elsevier, 2012, vol. 2.
- 11 B. Saparov and D. B. Mitzi, *Chem. Rev.*, 2016, **116**, 4558–4596.

- 12 X. Huang, J. Li and H. Fu, *J. Am. Chem. Soc.*, 2000, **122**, 8789–8790.
- 13 X. Huang, J. Li, Y. Zhang and A. Mascarenhas, *J. Am. Chem. Soc.*, 2003, **125**, 7049–7055.
- 14 X. Fang, M. Roushan, R. Zhang, J. Peng, H. Zeng and J. Li, *Chem. Mater.*, 2012, **24**, 1710–1717.
- 15 M. Roushan, X. Zhang and J. Li, *Angew. Chem.*, 2012, **124**, 451–454.
- 16 Z.-P. Wang, J.-Y. Wang, J.-R. Li, M.-L. Feng, G.-D. Zou and X.-Y. Huang, *Chem. Commun.*, 2015, **51**, 3094–3097.
- 17 C. Zhou, H. Lin, Y. Tian, Z. Yuan, R. Clark, B. Chen, L. J. van de Burgt, J. C. Wang, Y. Zhou, K. Hanson, Q. J. Meisner, J. Neu, T. Besara, T. Siegrist, E. Lambers, P. Djurovich and B. Ma, *Chem. Sci.*, 2018, **9**, 586–593.
- 18 A. Khan, A. Zeb, L. Li, W. Zhang, Z. Sun, Y. Wang and J. Luo, *J. Mater. Chem. C*, 2018, **6**, 2801–2805.
- 19 Z. Wang, Z. Zhang, L. Tao, N. Shen, B. Hu, L. Gong, J. Li, X. Chen and X. Huang, *Angew. Chem., Int. Ed.*, 2019, **58**, 9974–9978.
- 20 C. Zhou, M. Worku, J. Neu, H. Lin, Y. Tian, S. Lee, Y. Zhou, D. Han, S. Chen, A. Hao, P. I. Djurovich, T. Siegrist, M.-H. Du and B. Ma, *Chem. Mater.*, 2018, **30**, 2374–2378.
- 21 Z. Li, Y. Li, P. Liang, T. Zhou, L. Wang and R.-J. Xie, *Chem. Mater.*, 2019, **31**, 9363–9371.
- 22 W. Liu, Y. Fang and J. Li, *Adv. Funct. Mater.*, 2018, **28**, 1705593.
- 23 W. Liu, Y. Fang, G. Z. Wei, S. J. Teat, K. Xiong, Z. Hu, W. P. Lustig and J. Li, *J. Am. Chem. Soc.*, 2015, **137**, 9400–9408.
- 24 W. Liu, K. Zhu, S. J. Teat, G. Dey, Z. Shen, L. Wang, D. M. O'Carroll and J. Li, *J. Am. Chem. Soc.*, 2017, **139**, 9281–9290.
- 25 Z. Yuan, C. Zhou, Y. Tian, Y. Shu, J. Messier, J. C. Wang, L. J. van de Burgt, K. Kountouriotis, Y. Xin, E. Holt, K. Schanze, R. Clark, T. Siegrist and B. Ma, *Nat. Commun.*, 2017, **8**, 14051.
- 26 L. Mao, P. Guo, M. Kepenekian, I. Hadar, C. Katan, J. Even, R. D. Schaller, C. C. Stoumpos and M. G. Kanatzidis, *J. Am. Chem. Soc.*, 2018, **140**, 13078–13088.
- 27 L. Mao, Y. Wu, C. C. Stoumpos, M. R. Wasielewski and M. G. Kanatzidis, *J. Am. Chem. Soc.*, 2017, **139**, 5210–5215.
- 28 X. Zhang, W. Liu, G. Z. Wei, D. Banerjee, Z. Hu and J. Li, *J. Am. Chem. Soc.*, 2014, **136**, 14230–14236.
- 29 H. Barkaoui, H. Abid, A. Yangui, S. Triki, K. Boukheddaden and Y. Abid, *J. Phys. Chem. C*, 2018, **122**, 24253–24261.
- 30 L. Dou, A. B. Wong, Y. Yu, M. Lai, N. Kornienko, S. W. Eaton, A. Fu, C. G. Bischak, J. Ma, T. Ding, N. S. Ginsberg, L.-W. Wang, A. P. Alivisatos and P. Yang, *Science*, 2015, **349**, 1518–1521.
- 31 A. Khan, S. Han, X. Liu, K. Tao, D. Dey, J. Luo and Z. Sun, *Inorg. Chem. Front.*, 2018, **5**, 3028–3032.
- 32 Y. Li, Z. Xu, X. Liu, K. Tao, S. Han, Y. Wang, Y. Liu, M. Li, J. Luo and Z. Sun, *Inorg. Chem.*, 2019, **58**, 6544–6549.
- 33 G. A. Mousdis, N.-M. Ganotopoulos, H. Barkaoui, Y. Abid, V. Psycharis, A. Savvidou and C. P. Raptopoulou, *Eur. J. Inorg. Chem.*, 2017, 3401–3408.